Received November 1999
Revised March 2000
Accepted March 2000

Effects of heat generation/absorption and thermophoresis on hydromagnetic flow with heat and mass transfer over a flat surface

Ali J. Chamkha
Department of Mechanical and Industrial Engineering, Kuwait University, Kuwait and
Camille Issa
Department of Civil Engineering, Lebanese American University, Byblos, Lebanon

Keywords *Heat transfer, Hydromagnetics, Flow*

Abstract *The problem of steady, two-dimensional, laminar, hydromagnetic flow with heat and mass transfer over a semi-infinite, permeable flat surface in the presence of such effects as thermophoresis and heat generation or absorption is considered. A similarity transformation is used to reduce the governing partial differential equations into ordinary ones. The obtained self-similar equations are then solved numerically by an implicit, tri-diagonal, finite-difference scheme. Favourable comparison with previously published work is performed. Numerical results for the velocity, temperature and concentration profiles as well as for the skin-friction coefficient, wall heat transfer and particle deposition rate are obtained and reported graphically for various parametric conditions to show interesting aspects of the solution.*

Nomenclature

B = magnetic induction
c = particle concentration
c_p = fluid specific heat at constant pressure
C = Cunningham correction factor
C_f = skin-friction coefficient, $\mathrm{Re}_x^{-1/2} f''(0)$
C_m,
C_s, C_t = constants in equation (7)
D = diffusion coefficient
Ec = Eckert number, $u_\infty/(c_p(T_w - T_\infty))$
f = dimensionless stream function, $\psi/(2u_\infty vx)^{1/2}$
f_o = dimensionless wall mass transfer coefficient, $2v_o(x/(2vu_\infty))^{1/2}$
Ha = Hartmann number, $(2\sigma B^2/(\rho u_\infty))^{1/2}$
J_s = wall particle flux defined in equation (17)
Kn = Knudsen number
Nu_x = local Nusselt number, $-\mathrm{Re}_x^{1/2}\theta'(0)/2$
Pr = Prandtl number, $\mu c_p/\lambda_g$
q_w = wall heat transfer defined in equation (16)
Q_o = heat generation or absorption coefficient
Re_x = local Reynolds number, $2u_\infty x/\nu$
Sc = Schmidt number, ν/D
St_x = local Stanton number, $\mathrm{Re}_x^{-1/2}\phi'(0)/\mathrm{Sc}$
T = temperature
u,v = horizontal and vertical velocity components, respectively
v_o = wall suction or blowing velocity
V_T = thermophoretic velocity
x,y = horizontal and vertical coordinates, respectively.

Greek symbols
Δ = dimensionless heat generation or absorption coefficient, $2Q_o/(\rho c_p u_\infty)$

International Journal of Numerical Methods for Heat & Fluid Flow, Vol. 10 No. 4, 2000, pp. 432-448.

η = similarity parameter, $y/(u_\infty/2vx)^{1/2}$)
ϕ = dimensionless concentration, c/c_∞
κ = thermophoretic coefficient defined by equation (7)
λ_g, λ_p = thermal conductivity of fluid and diffused particles, respectively.
μ = dynamic viscosity
ν = kinematic viscosity
ρ = fluid density
τ = thermophoretic parameter defined by equation (8)
τ_f = wall shears stress defined in equation (15)
θ = dimensionless temperature $(T - T_\infty)/(T_w - T_\infty)$
σ = fluid electrical conductivity
ψ = stream function

Subscripts
∞ = free stream
w = wall

Introduction

Deposition of particles from a fluid-particle mixture is a subject which attracted many investigators due to its application in many engineering and natural processes. These include environmental and atmospheric pollution, filtration, sedimentation of particles on gas turbine blades, nuclear reactor safety, particulate deposition on semi-conductor wafers in the electronic industry and others. Deposition of particles on surfaces takes place by several mechanisms such as Brownian diffusion, impaction, interception, sedimentation and other field effects such as the electrostatic effects. As mentioned by Yiantsios and Karabelas (1998), the particle size is a very important parameter for the particle transport from the bulk of a flowing mixture and its attachment to the surface. For example, for mixtures with particles in the colloidal size range, Brownian diffusion controls the transport rate, while for mixtures with particles of much larger sizes ($> 10\mu$m) the particle inertia causes it to detach from the fluid streamlines and impact the surface. Prieve and Ruckenstein (1974) analyzed flow external to spheres as a model for deep-bed filtration. The effects of sedimentation for particulate deposition in rectilinear flows over flat surfaces were considered by Adamczyk and van de Ven (1981, 1982) and by Marmur and Ruckenstein (1986) for the deposition of cells on a flat plate. The problem of particulate deposition from a high temperature gas-particle flow with no hydrodynamic interaction on to an adjacent cold flat surface was studied previously by many investigators such as Goren (1977), Homsy *et al.* (1981), Mills *et al.* (1984) and Batchelor and Shen (1985). All of these investigators produced numerical solutions for the flow and temperature fields and then obtained the particle deposition rate in the presence of thermophoresis. Gokoglu and Rosner (1984a) and Tsai (1999) reported correlations for predicting the deposition rate in the presence of thermophoresis. Jia *et al.* (1992) investigated numerically the interaction between radiation and thermophoresis in forced convection laminar boundary-layer flow. The effect of thermophoresis on laminar flow over cold inclined plate with variable properties was reported by Jayaraj (1995). Natural convection laminar flow over a cold vertical flat plate in the presence of thermophoresis was solved numerically by Jayaraj (1999) and Jayaraj *et al.* (1999) for constant and variable properties, respectively. Chiou (1998) analyzed the effect of thermophoresis on submicron particle deposition

from a forced laminar boundary layer flow on to an isothermal moving plate through similarity solutions. The same problem was studied on a vertical isothermal cylinder by Chiou and Cleaver (1996). The effect of particulate thermophoresis in reducing the fouling rate advantages of effusion-cooling was analyzed by Gokoglu and Rosner (1984b). Also, the thermophoretic deposition of small particles in laminar tube flow was considered by Walker *et al.* (1979).

In certain applications such as those dealing with chemical reactions and dissociating fluids, possible heat generation or absorption effects may alter the temperature distribution and, therefore, the particle deposition rate. This may occur in such applications related to nuclear reactors, electronic chips, and semi-conductor wafers. Previous investigations dealing with temperature-dependent heat sources or sinks for different geometries can be found in the works of Sparrow and Cess (1961), Vajravelu and Nayfeh (1992), Vajravelu and Hadjinicolaou (1997) and Chamkha (1999).

The use of electrically-conducting fluids under the influence of magnetic fields has gained interest in various industrial applications such as the semi-conductor industries and the purification of molten metals from non-metallic inclusions. In certain fluid-particle mixtures, the fluid phase may be electrically conducting. For such situations, the presence of a magnetic field influences the flow and thermal behavior of the suspension which, in turn, impacts the particle deposition rate considerably. Some examples of investigations dealing with hydromagnetic flows over a surface can be found in the work of Chakrabarti and Gupta (1979), Chiam (1995), Chandran *et al.* (1996) and Vajravelu and Hadjinicolaou (1997).

The purpose of this work is to consider the effects of heat generation or absorption and thermophoresis on steady, laminar, hydromagnetic, two-dimensional flow with heat and mass transfer over a semi-infinite, permeable flat surface.

Governing equations

Consider steady, laminar, two-dimensional boundary-layer flow with heat and mass transfer over a semi-infinite, permeable flat surface. The flow takes place in the positive xy plane with the surface being at the plane $y = 0$. The surface is maintained at a constant temperature T_w and allows for possible non-uniform wall suction or blowing. A heat source/sink is placed within the flow to allow for possible heat generation/absorption effects. In addition, the effect of thermophoresis is taken into account as it helps in understanding mass deposition on surfaces. The fluid is assumed to be Newtonian, electrically conducting and heat generating/absorbing. A non-uniform magnetic field is applied in the vertical y direction normal to the flow direction. The governing equations for this physical situation are based on the usual balance laws of mass, linear momentum, energy and mass diffusion modified to account for the physical effects mentioned above. These equations are given by

$$\frac{\partial u}{\partial x} + \frac{\partial v}{\partial y} = 0 \tag{1}$$

$$u\frac{\partial u}{\partial x}+v\frac{\partial u}{\partial y}=\nu\frac{\partial^2 u}{\partial y^2}-\frac{\sigma B^2(x)}{\rho}(u-u_\infty) \tag{2}$$

$$u\frac{\partial T}{\partial x}+v\frac{\partial T}{\partial y}=\frac{\lambda_g}{\rho c_p}\frac{\partial^2 T}{\partial y^2}+\frac{\mu}{\rho c_p}\left(\frac{\partial u}{\partial y}\right)^2+\frac{\sigma B^2}{\rho c_p}(u-u_\infty)^2 + \frac{Q_o}{\rho c_p}(T-T_\infty) \tag{3}$$

$$u\frac{\partial c}{\partial x}+v\frac{\partial c}{\partial y}=D\frac{\partial^2 c}{\partial y^2}-\frac{\partial}{\partial y}(V_T c) \tag{4}$$

where x and y are the horizontal and vertical directions, respectively; u, v and T are the fluid x-component (horizontal) of velocity, y-component (vertical) of velocity, and temperature, respectively. c is the mass or particle concentration in the fluid; $\rho, \mu, \nu, \lambda_g, c_p$, and σ are the fluid density, dynamic viscosity, kinematic viscosity, thermal conductivity, specific heat at constant pressure and electrical conductivity, respectively; $B(x)$ and Q_o are the magnetic induction and heat generation/absorption coefficient, respectively; D and V_T are the diffusion coefficient and the thermophoretic velocity, respectively; u_∞ and T_∞ are the free stream velocity and temperature, respectively.

The boundary conditions for this problem can be written as

$$\begin{aligned} &u(x,0)=0, v(x,0)=-v_o(x), \quad T(x,0)=T_w, c(x,0)=c_w \\ &u(x,\infty)=u_\infty, \quad T(x,\infty)=T_\infty\ , \ c(x,\infty)=c_\infty \end{aligned} \tag{5}$$

where $v_o(x)$ is the wall suction (> 0) or blowing (< 0) velocity, T_w, c_w and c_∞ are the fluid wall temperature, wall mass concentration, and the free stream mass concentration, respectively.

In equation (4), the thermophoretic velocity V_T was given by Talbot *et al.* (1980) and later by Tsai (1999) as

$$V_T=-\kappa\nu\frac{\nabla T}{T}=-\frac{\kappa\nu}{T}\frac{\partial T}{\partial y} \tag{6}$$

where κ is the thermophoretic coefficient which ranges in value from 0.2 to 1.2 as indicated by Batchelor and Shen (1985) and is defined by

$$\kappa=\frac{2C_s(\lambda_g/\lambda_p+C_t\mathrm{Kn})C}{(1+3C_m\mathrm{Kn})(1+2\lambda_g/\lambda_p+2C_t\mathrm{Kn})} \tag{7}$$

where C_m, C_s, and C_t are constants, λ_g and λ_p are the thermal conductivities of the fluid and diffused particles, respectively. C is the Cunningham correction factor and Kn is the Knudsen number. A thermophoretic parameter τ can be defined as done previously by Mills *et al.* (1984) and Tsai (1999) as follows

$$\tau = \frac{\kappa(T_w - T_\infty)}{T} \tag{8}$$

Typical values of τ are 0.01, 0.1, and 1.0 corresponding to approximate values of $-\kappa(T_w - T_\infty)$ equal to 3, 30, and 300K for a reference temperature of 300K.

It is convenient to substitute the following similarity transformations

$$\eta = y\left(\frac{u_\infty}{2\nu x}\right)^{1/2}\ ,\ \psi = (2\nu u_\infty x)^{1/2} f(\eta)\ ,\ \theta = \frac{T - T_\infty}{T_w - T_\infty}, \phi = \frac{c}{c_\infty} \tag{9}$$

(where ψ is the stream function defined in the usual way such that $u = \frac{\partial \psi}{\partial y}, v = -\frac{\partial \psi}{\partial x}$) into equations (1) through (5) to yield

$$f''' + ff'' - \mathrm{Ha}^2(f' - 1) = 0 \tag{10}$$

$$\frac{1}{\mathrm{Pr}}\theta'' + f\theta' + \mathrm{Ec}(f'')^2 + \mathrm{Ec}\,\mathrm{Ha}^2(f' - 1)^2 + \Delta\theta = 0 \tag{11}$$

$$\frac{1}{\mathrm{Sc}}\phi'' + (f - \tau\theta')\phi' - \tau\theta''\phi = 0 \tag{12}$$

$$\begin{aligned} &f'(0) = 0\ ,\ f(0) = f_o\ ,\ \theta(0) = 1,\ \phi(0) = 0 \\ &f'(\infty) = 1\ ,\ \theta(\infty) = 0\ ,\ \phi(\infty) = 1 \end{aligned} \tag{13}$$

where a prime denotes ordinary differentiation with respect to η, $f_o = 2v_o(x/(2\nu u_\infty))^{1/2}$ is the dimensionless wall mass transfer coefficient such that $f_o > 0$ indicates wall suction and $f_o < 0$ indicates wall injection and

$$\begin{aligned} \mathrm{Ha}^2 &= \frac{2\sigma B^2}{\rho u_\infty}\ ,\ \mathrm{Pr} = \frac{\mu c_p}{k}\ ,\ \mathrm{Ec} = \frac{u_\infty}{c_p(T_w - T_\infty)} \\ \Delta &= \frac{2Q_o}{\rho c_p u_\infty}\ ,\ Sc = \frac{\nu}{D} \end{aligned} \tag{14}$$

are the square of the Hartmann number, Prandtl number, Eckert number, dimensionless heat generation or absorption coefficient, and the Schmidt number, respectively. It should be noted that for a similarity solution f_o must be constant. For this condition to be satisfied, v_o must be proportional to $x^{-1/2}$.

The skin-friction coefficient, wall heat transfer coefficient (or local Nusselt number) and the wall deposition flux (or the local Stanton number) are important physical parameters. These can be defined as

$$C_f = \frac{\tau_f}{\rho u_\infty^2} = \mathrm{Re}_x^{-1/2} f''(0)\ ;\ \tau_f = \mu \left.\frac{\partial u}{\partial y}\right|_{y=0} \tag{15}$$

$$\mathrm{Nu}_x = \frac{q_w x}{(T_w - T_\infty)k} = -\frac{1}{2}\mathrm{Re}_x^{1/2}\theta'(0) \; ; \; q_w = -k\left.\frac{\partial T}{\partial y}\right|_{y=0} \tag{16}$$

$$\mathrm{St}_x = \frac{-J_s}{u_\infty c_\infty} = \frac{1}{\mathrm{Sc}}\mathrm{Re}_x^{-1/2}\phi'(0) \; ; \; J_s = -D\left.\frac{\partial c}{\partial y}\right|_{y=0} \tag{17}$$

where $\mathrm{Re}_x = 2u_\infty x/\nu$ is the local Reynolds number.

Numerical method

Equations (10) through (12) represent the transformed similarity equations of the governing momentum, energy, and concentration equations, respectively. They are solved numerically by an implicit, iterative, tri-diagonal finite-difference method similar to that discussed by Blottner (1970).

The third-order differential equation (10) is converted into a second-order one by substituting $V = f'$. Then, all second-order equations for V, θ, and ϕ are discretized using three-point central difference quotients while the first-order differential equation $V = f'$ is discretized by the trapezoidal rule. As a consequence, a set of algebraic equations results. With the non-linear terms evaluated at the previous iteration, the algebraic equations are solved with iteration by the well-known Thomas algorithm (see Blottner, 1970). It is expected that the largest changes in the dependent variables occur in the region close to the surface. A small step size is needed there to accurately approximate the derivatives numerically. On the other hand, away from the surface small changes in the dependent variables are expected. Therefore, a large step size may be used there. For this reason, a variable step size scheme was employed. The initial step size $\Delta\eta_1$ was equal to 0.001 and the growth factor G was equal to 1.03 such that $\Delta\eta_{i+1} = G\Delta\eta_i$. The employed computational domain consisted of 196 grid points. This gave $\eta_\infty = 10.3$ as representing the position at infinity. This value of η was proved to be satisfactory for all conditions considered in this work ranging from small values of Sc (thick concentration boundary layer) to very large values of Sc (thin concentration boundary layer). A convergence criterion based on the relative difference between the current and the previous iterations was employed. When this difference reached 10^{-7}, the solution was assumed converged and the iteration process was terminated. A representative set of numerical results is shown graphically in Figures 1 to 14 to illustrate the influence of the various physical parameters on the solution.

Table I presents a comparison of the local Stanton number ($\mathrm{St}_x\ \mathrm{Re}_x^{1/2}\sqrt{2}$) obtained in the present work and those obtained earlier by Mills *et al.* (1984) and Tsai (1999). It is clearly observed that good agreement between the results exists. This lends confidence in the numerical method.

τ	f_o	Mills *et al.* (1984)	Tsai (1999)	Present work
0.01	1.0	0.7091	0.7100	0.7093
0.01	0.5	0.3559	0.3565	0.3590
0.01	0	0.0029	0.0029	0.0030
0.1	1.0	0.7265	0.7346	0.7241
0.1	0.5	0.3767	0.3810	0.3810
0.1	0	0.0277	0.0275	0.0280
0.1	–0.004	0.0249	0.0246	0.0246
0.1	–0.005	0.0242	0.0239	0.0241
1.0	1.0	0.8619	0.9134	0.8932
1.0	0.5	0.5346	0.5598	0.5450
1.0	0	0.2095	0.2063	0.2120
1.0	–0.004	0.2068	0.2034	0.2073
1.0	–0.005	0.2062	0.2027	0.2070
1.0	–0.250	0.0344	0.0295	0.0350

Table I.
Comparison of $St_x\ Re_x^{1/2}\sqrt{2}$ with those of Mills *et al.* (1984) and Tsai (1999) for $Sc \geq 1{,}000$, $Ec = 0$, $Ha = 0$, $Pr = 0.7$ and $\Delta = 0$

Results and discussion

In this section, a comprehensive numerical parametric study is conducted and the results are reported in terms of graphs. This is done in order to illustrate special features of the solutions.

Figures 1 to 3 present typical profiles for the velocity, temperature and concentration for various values of the Hartmann number Ha, respectively for a physical situation with heat generation and thermophoretic effect. Application of a magnetic field moving with the free stream has the tendency to induce a

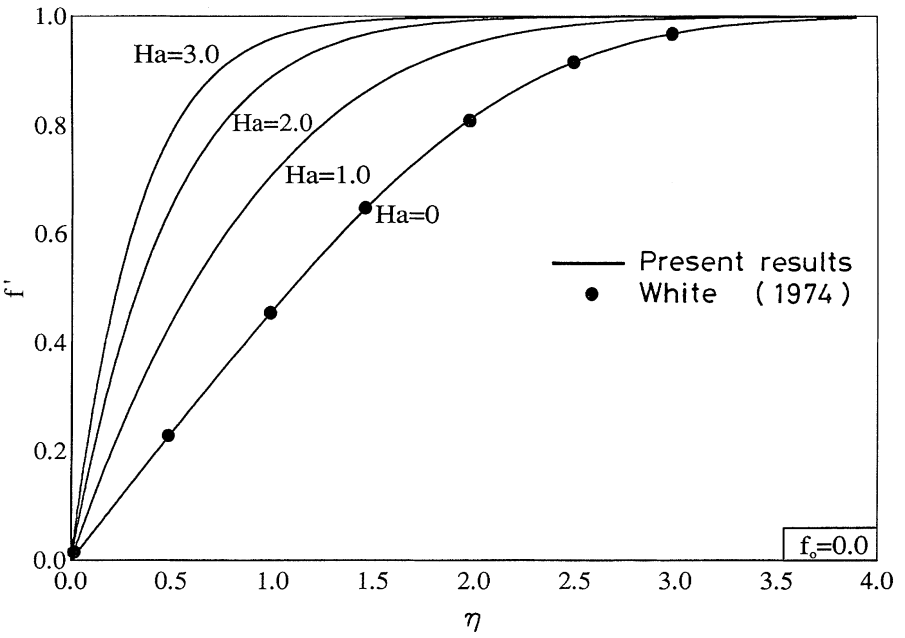

Figure 1.
Effects of Ha on velocity profiles

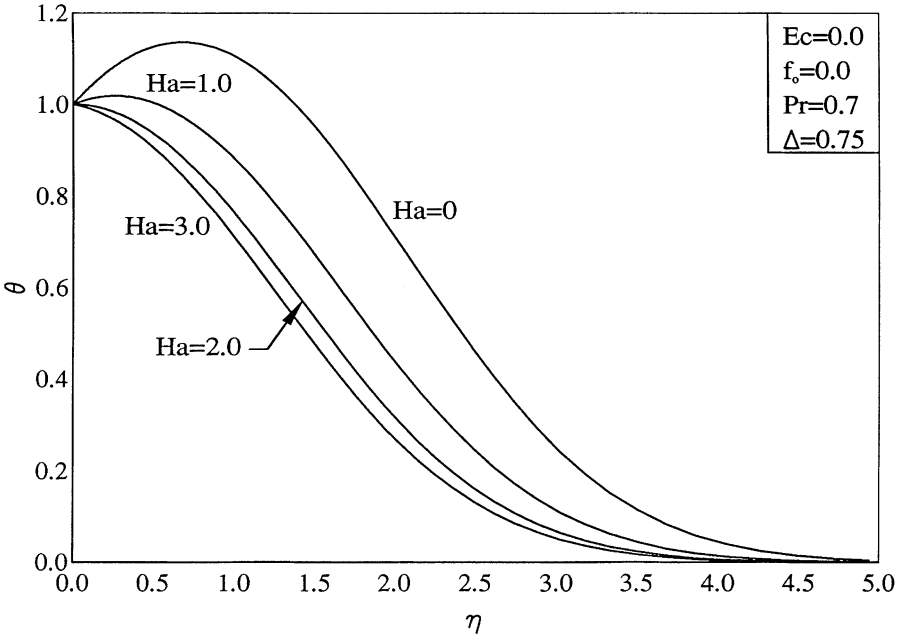

Figure 2.
Effects of Ha on temperature profiles

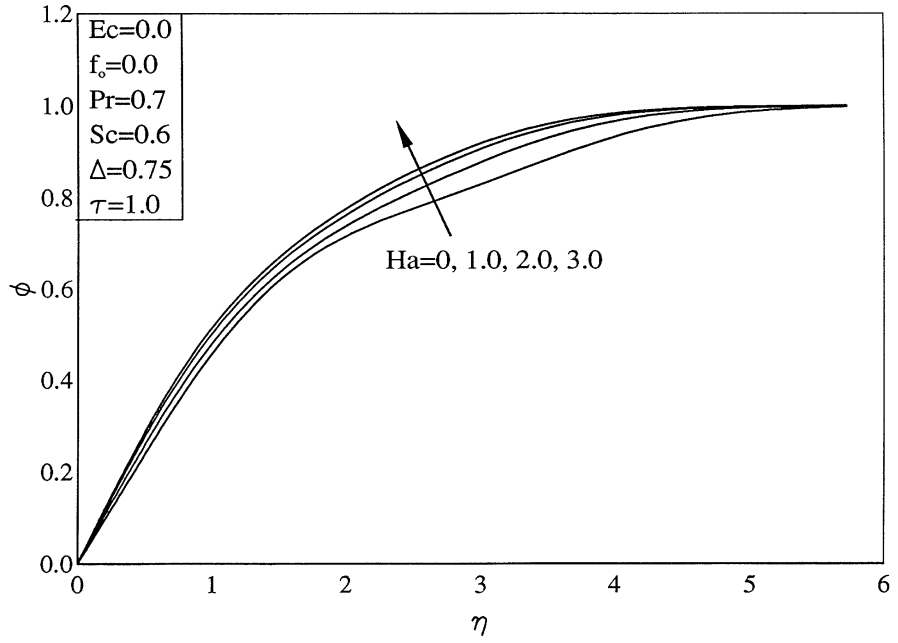

Figure 3.
Effects of Ha on concentration profiles

motive force which increases the motion of the fluid and decreases its boundary layer. This is accompanied by a decrease in the fluid temperature and a slight increase in the concentration. In addition, the thermal boundary layer decreases

as a result of increasing the strength of the magnetic field. Inspection of Figure 2 shows that a distinctive peak in the fluid temperature occurs in the fluid close to the boundary and not at the surface. This is due to the presence of the heat generation effect ($\Delta = 0.75$) used to obtain this Figure. It is seen that this peak value diminishes as the Hartmann number increases. This and all previous facts are clearly shown in Figures 1 to 3. It should be noted that in the absence of the magnetic field (Ha = 0), the velocity profile f' is in excellent agreement with the Blasius solution for boundary-layer flow over a flat plate reported by White (1974).

Figures 4 to 6 illustrate the influence of the wall mass transfer coefficient f_o on the velocity, temperature, and concentration profiles, respectively. Imposition of wall fluid suction ($f_o > 0$) for this problem has the effect of reducing all of the hydrodynamic, thermal and concentration boundary layers causing the fluid velocity and its concentration to increase while decreasing its temperature. On the other hand, imposition of wall fluid injection or blowing produces the opposite effect, namely decreases in the fluid velocity and concentration and an increase in its temperature. These effects are accompanied by increases in all of the hydrodynamic, thermal and concentration boundary layers.

Figure 7 depicts the influence of the dimensionless heat generation or absorption coefficient δ on the fluid temperature profile. As mentioned before, owing to the presence of a heat source or a heat generation effect ($\Delta > 0$), the thermal state of the fluid increases causing the thermal boundary layer to increase. In the event that the strength of the heat source is relatively large, the maximum fluid temperature does not occur at the wall but rather in the

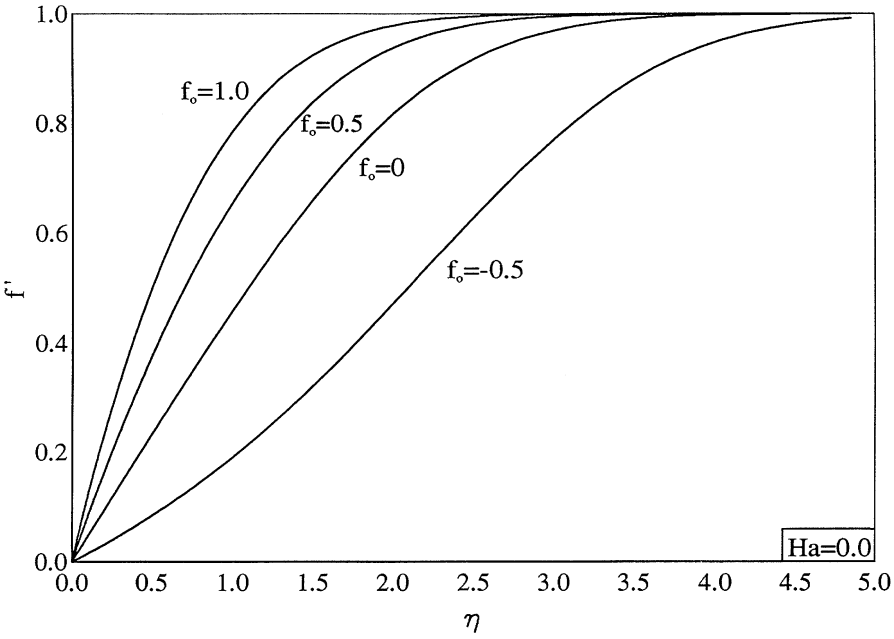

Figure 4.
Effects of f_o on velocity profiles

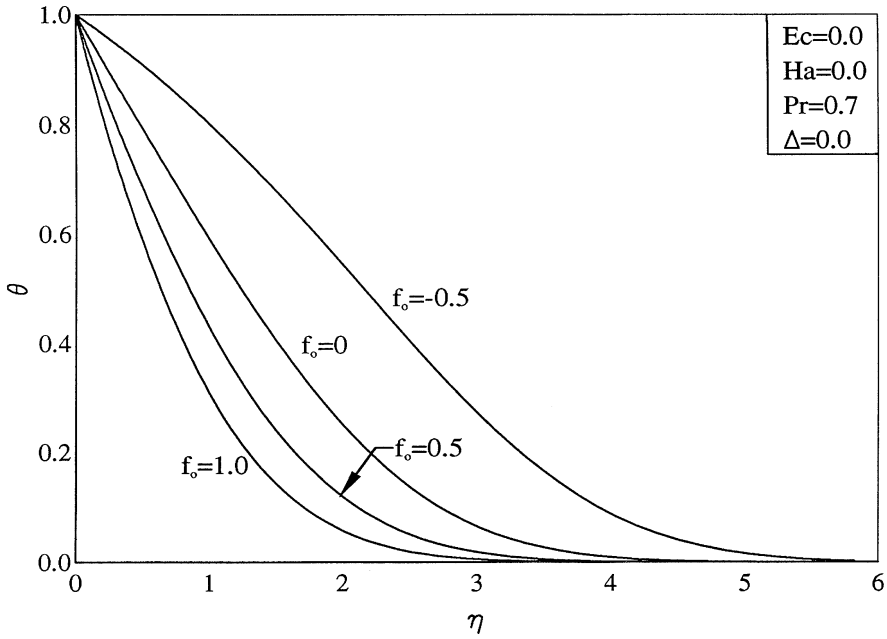

Figure 5.
Effects of f_o on temperature profiles

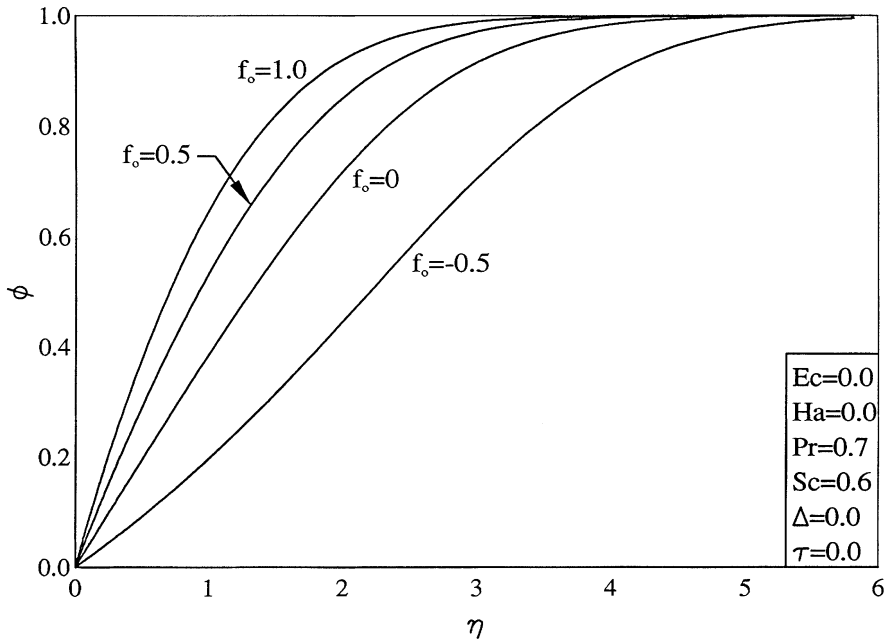

Figure 6.
Effects of f_o on concentration profiles

fluid region close to it. Conversely, the presence of a heat sink or a heat absorption effect ($\Delta < 0$) causes a reduction in the thermal state of the fluid, thus producing lower thermal boundary layers. These facts are obvious from Figure 7.

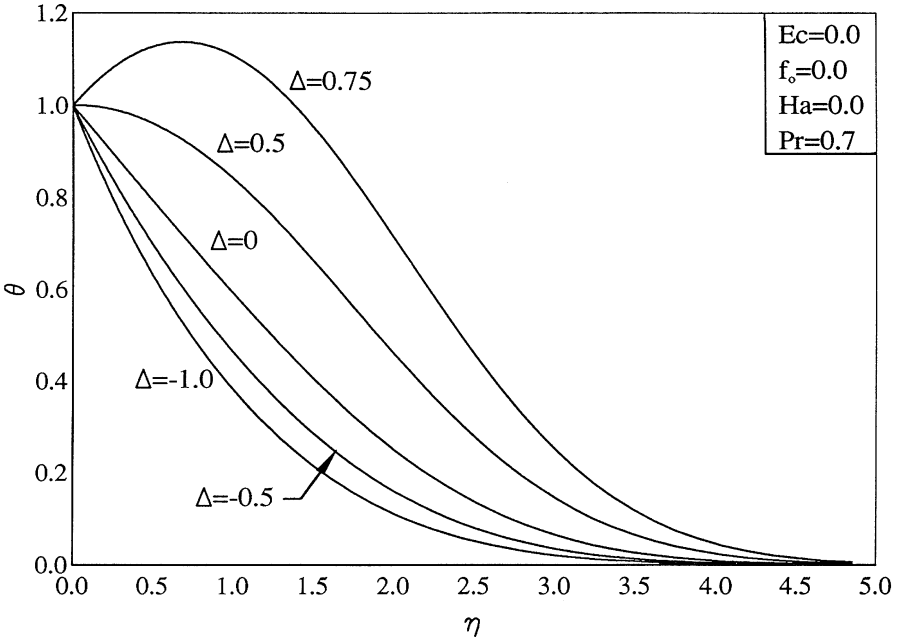

Figure 7.
Effects of Δ on temperature profiles

Figures 8 and 9 show typical concentration profiles for various values of the Schmidt number Sc and the thermophoretic parameter τ, respectively. It is clear that the concentration boundary layer decreases while the concentration

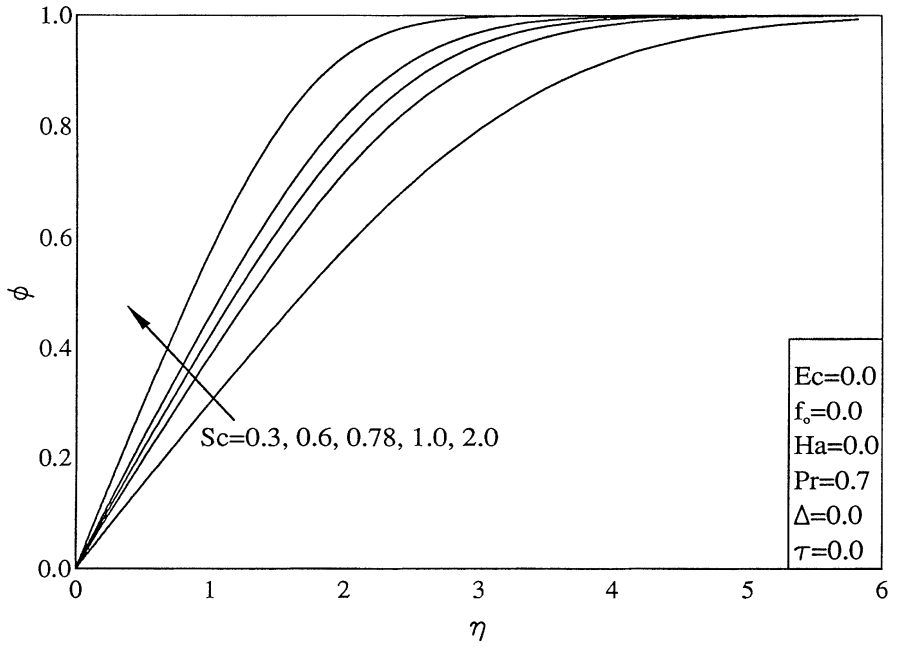

Figure 8.
Effects of Sc on concentration profiles

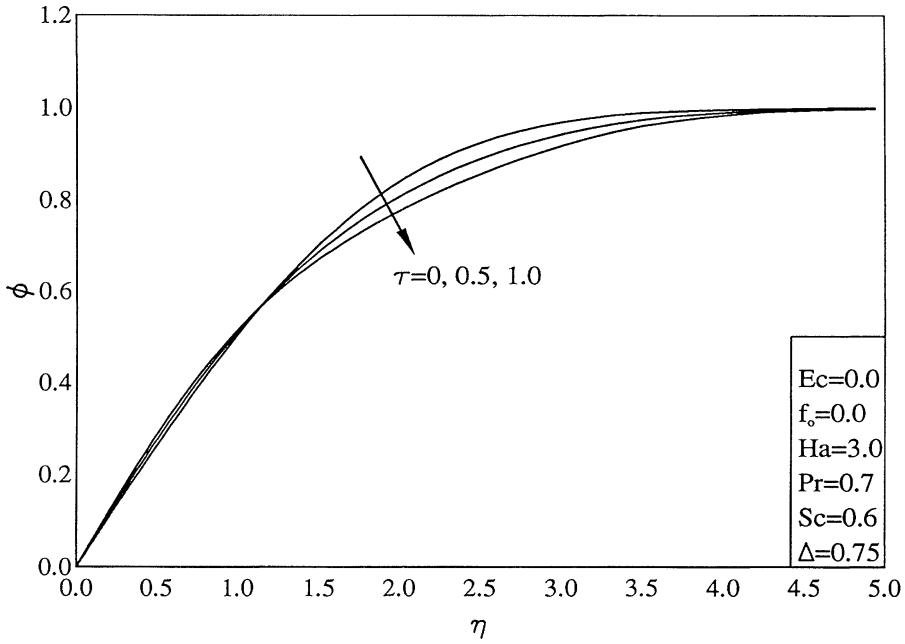

Figure 9.
Effects of τ on concentration profiles

increases as the Schmidt number Sc increases. However, for the parametric conditions used in Figure 9, the effect of increasing the thermophoretic parameter τ is limited to increasing the wall slope of the concentration profile and decreasing the concentration for values of $\eta > 1.0$ without any significant effect on the concentration boundary layer. This is true only for small values of Sc for which the Brownian diffusion effect is large compared to the convection effect. However, for large values of Sc (Sc > 1,000) the diffusion effect is minimal compared to the convection effect and, therefore, the thermophoretic parameter τ is expected to alter the concentration boundary layer significantly. This is consistent with the work of Goren (1977) on thermophoresis of aerosol particles in flat-plate boundary layer.

The relative influence of both the viscous and magnetic dissipations on the fluid temperature and concentration profiles was also investigated but the results are not presented herein for brevity. It was observed from these results that the temperature distribution increased while the concentration distribution decreased slightly as a result of the viscous dissipation effect which acts as a heat source. In addition, the magnetic dissipation (or Joule heating) effect which acts as a heat sink was seen to decrease the temperature distribution and to increase the concentration distribution slightly.

In Figures 10 to 12, the effects of f_o, Ha and Ec on the skin-friction coefficient $C_f \mathrm{Re}_x^{1/2}(f''(0))$, the wall heat transfer $2\mathrm{Nu}_x \mathrm{Re}_x^{-1/2}(-\theta'(0))$, and the wall deposition flux $\mathrm{St}_x \mathrm{Sc} \mathrm{Re}_x^{1/2}(\phi'(0))$ are, respectively, presented. Inspection of Figures 1 and 4 shows that the wall slope of the velocity profile increases with increases in either of f_o or Ha. This is consistent with Figure 10. Also, since

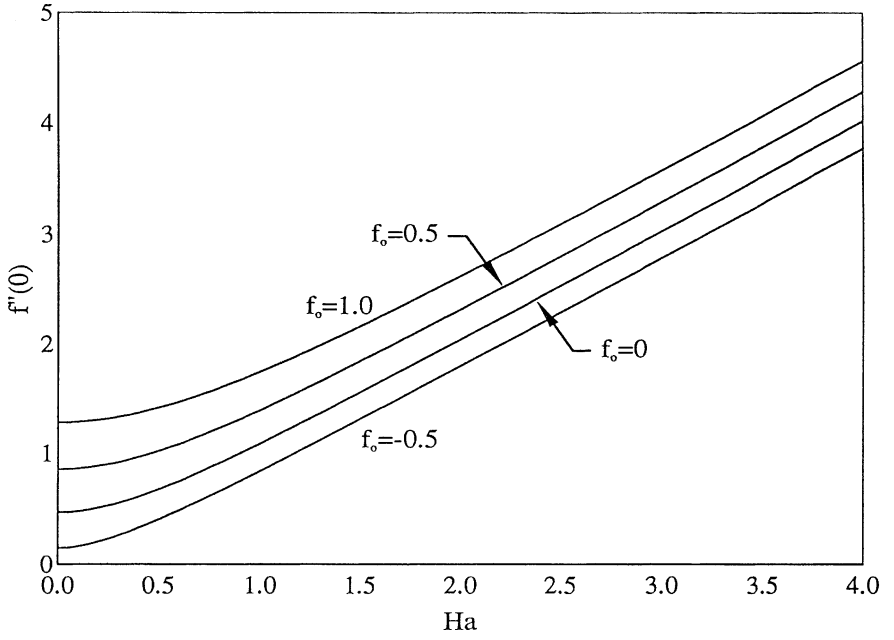

Figure 10.
Effects of f_o and Ha on sking-friction coefficients

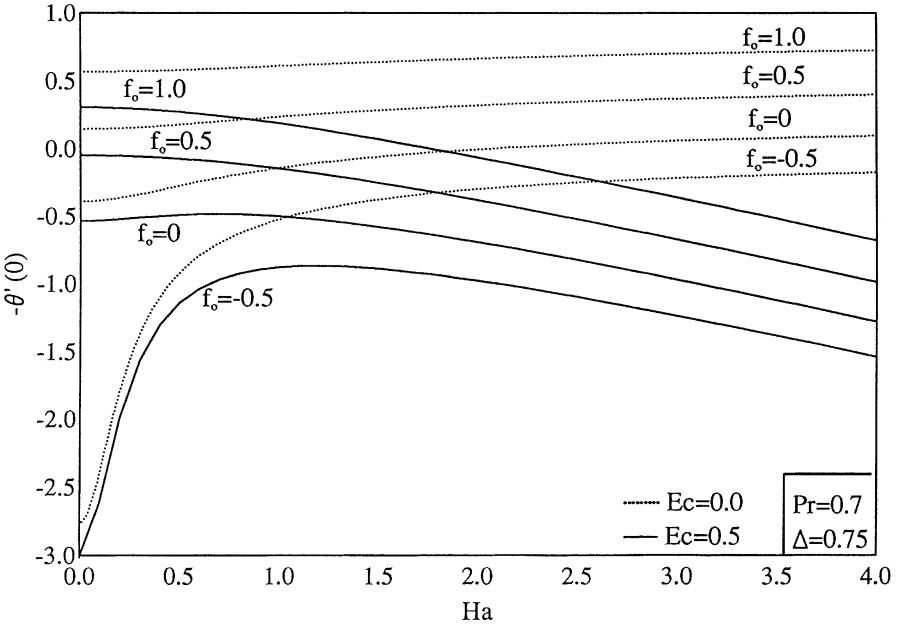

Figure 11.
Effects of Ha, Ec, f_o and Ha on wall heat transfer

equation (10) is uncoupled from equations (11) and (12), Ec has no influence on $f''(0)$. However, inspection of Figures 2 and 5 shows that the wall slope of the temperature profile decreases with increases in either f_o or Ha. This means that the wall heat temperature increases as either f_o or Ha increases as is the case in

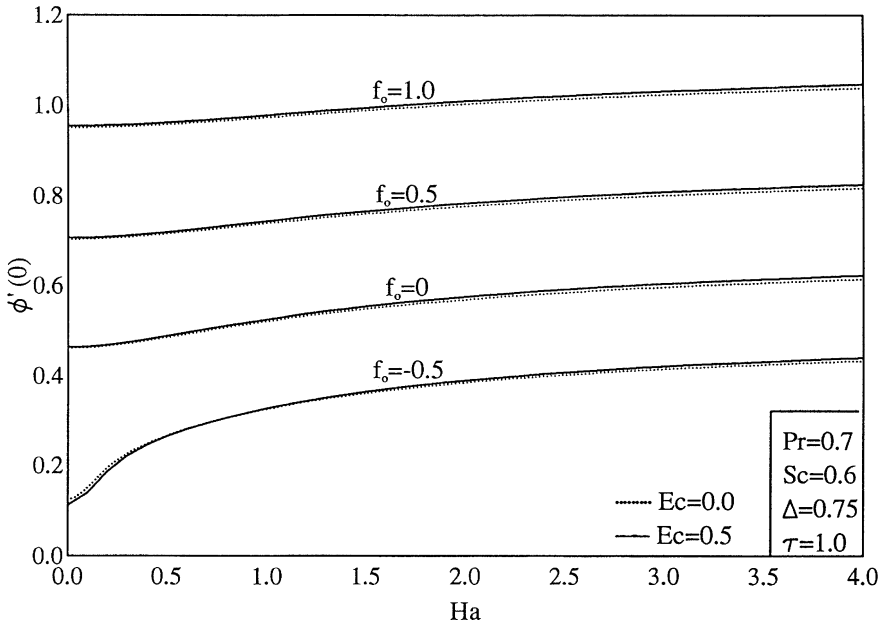

Figure 12.
Effects of Ec, f_o and Ha on wall deposition flux

Figure 11. Also, it was observed from other results not presented herein that $(\theta'(0))$ increases due to the presence of the viscous dissipation (Ec $\neq$ 0, Ha = 0) effect and decreases due to the Joule heating effect (Ec $\neq$ 0, Ha $\neq$ 0) in the absence of viscous dissipation. This produces decreases in the wall heat transfer for all conditions since the viscous dissipation is present as is evident from Figure 11 except in the case of fluid injection ($f_o < 0$) where the wall heat transfer increases and then decreases as the value of Ha is increased. Similar conclusions can be reached by inspection of Figures 3 and 6 where the wall deposition flux is increased as either f_o or Ha is increased for Ec = 0 and it is increased slightly as Ha is increased for Ec $\neq$ 0 as shown in Figure 12.

Finally, Figures 13 and 14 display the influence of the Prandtl number Pr, Δ and τ on the wall heat transfer and the wall deposition flux, respectively in the absence of both viscous and magnetic dissipations. Again, by inspection of Figures 7 and 9, it can be concluded that the wall heat transfer decreases with heat generation while it increases with heat absorption and that the wall deposition flux increases as either τ or Δ is increased. Also, it can be seen from Figure 13 that the wall heat transfer increases with Pr for $\Delta \leq 0$ and decreases for $\Delta > 0$. In addition, the wall deposition flux increases with Pr for $\Delta > 0$ while it increases then decreases for $\Delta \leq 0$ and $\tau = 1.0$ (forming a distinctive peak for small values of Pr) or remains constant with Pr for $\Delta \leq 0$ and $\tau = 0.1$ as is evident from Figure 14.

Conclusion

This work considered the effects of wall suction or injection, heat generation or absorption, thermophoresis, and magnetic field on steady, laminar flow with heat and mass transfer of an electrically-conducting fluid over a semi-infinite, porous

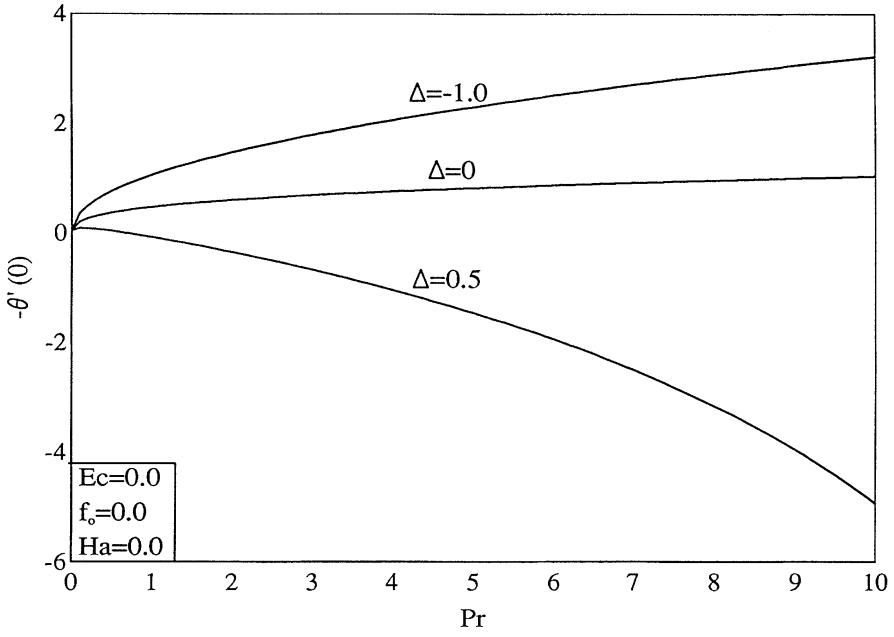

Figure 13.
Effects of Pr and Δ on wall heat transfer

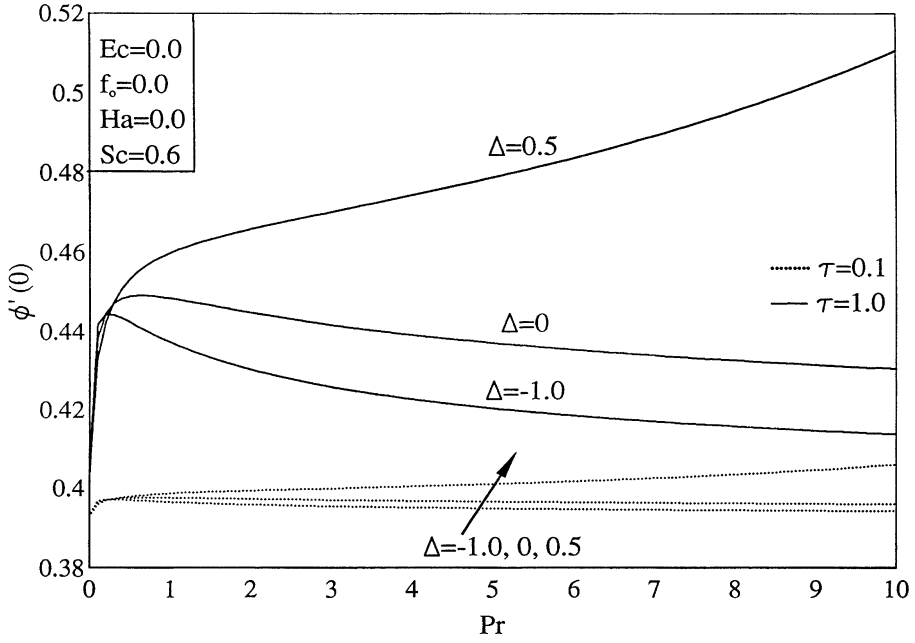

Figure 14.
Effects of Pr, Δ and τ on wall deposition flux

flat surface. A set of similarity equations governing the fluid velocity and temperature and the particle mass concentration was obtained by using a similarity transformation. An implicit tri-diagonal finite-difference method was successfully employed for the solution of the resulting coupled ordinary

differential equations. Comparisons with previously published work were performed and the results were found to be in good agreement. A comprehensive set of graphical results for the velocity, temperature, and concentration as well as the skin-friction coefficient, local Nusselt number, and the local Stanton number was presented and discussed. It was found that the local Nusselt number increased as either the wall suction velocity or the Hartmann number was increased and decreased due to the presence of either viscous dissipation or heat generation effects. Also, the local Stanton number was predicted to increase as the wall suction velocity, the Hartmann number, the thermophoresis effect or the heat generation effect was increased. It is hoped that the present work can be used as a vehicle for understanding the particle deposition phenomenon in the presence of a magnetic field and a heat source of a sink.

References

Adamczyk, Z. and van de Ven, T.G.M. (1981), "Deposition of particles under external forces in laminar flow through parallel-plate and cylindrical channels", *J. Colloid Interface Sci.*, Vol. 80, pp. 340-56.

Adamczyk, Z. and van de Ven, T.G.M. (1982), "Particle transfer to a plate in uniform flow", *Chem. Eng. Sci.*, Vol. 37, pp. 869-80.

Batchelor, G.K. and Shen, C. (1985), "Thermophoretic deposition of particles in gas flowing over cold surfaces", *J. Colloid Interface Sci.*, Vol. 107, pp. 21-37.

Blottner, F.G. (1970), "Finite-difference methods of solution of the boundary-layer equations", *AIAA Journal*, Vol. 8, pp. 193-205.

Chakrabarti, A. and Gupta, A.S. (1979), "Hydromagnetic flow and heat transfer over a stretching sheet", *Q. Appl. Math.*, Vol. 37, pp. 73-8.

Chamkha, A.J. (1999), "Hydromagnetic three-dimensional free convection on a vertical stretching surface with heat generation or absorption", *Int. J. Heat Fluid Flow*, Vol. 20, pp. 84-92.

Chandran, P., Sacheti, N.C. and Singh, A.K. (1996), "Hydromagnetic flow and heat transfer past a continuously moving porous boundary", *Int. Commun. Heat Mass Transfer*, Vol. 23, pp. 889-98.

Chiam, T.C. (1995), "Hydromagnetic flow over a surface stretching with a power-law velocity", *Int. J. Engng Sci.*, Vol. 33, pp. 429-35.

Chiou, M.C. (1998), "Effect of thermophoresis on sub-micron particle deposition from a forced laminar boundary layer flow on to an isothermal moving plate", *Acta Mechanica*, Vol. 129, pp. 219-29.

Chiou, M.C. and Cleaver, J.W. (1996), "Effect of thermophoresis on sub-micron particle deposition from a laminar forced convection boundary layer flow on to an isothermal cylinder", *Journal of Aerosol Science*, Vol. 27, pp. 1155-67.

Gokoglu, S.A. and Rosner, D.E. (1984a), "Correlation of thermophoretically-modified small particle diffusional deposition rates in forced convection systems with variable properties, transpiration cooling and/or viscous dissipation", *Int. J. Heat Mass Transfer*, Vol. 27, pp. 639-46.

Gokoglu, S.A. and Rosner, D.E. (1984b), "Effect of particulate thermophoresis in reducing the fouling rate advantages of effusion-cooling", *Int. J. Heat Fluid Flow*, Vol. 5, pp. 37-41.

Goren, S.L. (1977), "Thermophoresis of aerosol-particles in laminar boundary-layer on a flat-plate", *J. Colloid Interface Sci.*, Vol. 61, pp. 77-85.

Homsy, G.M., Geyling, F.T. and Walker, K.L. (1981), "Blasius series for thermophoretic deposition of small particles", *Colloid Interface Sci.*, Vol. 83, pp. 495-501.

Jayaraj, S. (1995), "Thermophoresis in laminar flow over cold inclined plates with variable properties", *Heat and Mass Transfer/Wärme-und Stoffüberträgung*, Vol. 30, pp. 167-73.

Jayaraj, S. (1999), "Finite difference modelling of natural convection flow with thermophoresis", *Int. J. of Numerical Methods for Heat & Fluid Flow*, Vol. 9, pp. 692-704.

Jayaraj, S., Dinesh, K.K. and Pillai, K.L. (1999), "Thermophoresis in natural convection with variable properties", *Heat and Mass Transfer/Waerme- und Stoffüberträgung*, Vol. 34, pp. 469-75.

Jia, G., Cipolla, J.W. and Yener, Y. (1992), "Thermophoresis of a radiating aerosol in laminar boundary-layer flow", *Journal of Thermophysics and Heat Transfer*, Vol. 6, pp. 476-82.

Marmur, A. and Ruckenstein, E. (1986), "Gravity and cell adhesion", *J. Colloid Interface Sci.*, Vol. 114, pp. 261-6.

Mills, A.F., Hang, X. and Ayazi, F. (1984), "The effect of wall suction and thermophoresis on aerosol-particle deposition from a laminar boundary-layer on a flat-plate", *Int. J. Heat Mass Transfer*, Vol. 27, pp. 1110-13.

Prieve, D.C. and Ruckenstein, E. (1974), "Effect of London forces upon the rate of deposition of Brownian particles", *A.I.Ch.E. J.*, Vol. 20, pp. 1178-87.

Sparrow, E.M. and Cess, R.D. (1961), "Temperature dependent heat sources or sinks in a stagnation point flow", *App. Sci. Res.*, Vol. A10, pp. 185-97.

Talbot, L., Cheng, R.K., Scheffer, R.W. and Wills, D.P. (1980), "Thermophoresis of particles in a heated boundary layer", *J. Fluid Mechanics*, Vol. 101, pp. 737-58.

Tsai, R. (1999), "A simple approach for evaluating the effect of wall suction and thermophoresis on aerosol particle deposition from a laminar flow over a flat plate", *Int. Commun. Heat Mass Transfer*, Vol. 26, pp. 249-57.

Vajravelu, K. and Hadjinicolaou, A. (1997), "Convective heat transfer in an electrically conducting fluid at a stretching surface with uniform free stream", *Int. J. Engng. Sci.*, Vol. 35, pp. 1237-44.

Vajravelu, K. and Nayfeh, J. (1992), "Hydromagnetic convection at a cone and a wedge", *Int. Commun. Heat Mass Transfer*, Vol. 19, pp. 701-10.

Walker, K.L., Homsy, G.M. and Geyling, F.T. (1979), "Thermophoretic deposition of small particles in laminar tube flow", *J. Colloid Interface Sci.*, Vol. 69, pp. 138-47.

White, F. (1974), *Viscous Fluid Flow*, 1st ed., McGraw-Hill, New York, NY, p. 265.

Yiantsios, S.G. and Karabelas, A.J. (1998), "The effect of gravity on the deposition of micron-sized particles on smooth surfaces", *Int. J. Multiphase Flow*, Vol. 24, pp. 283-93.